

# Modeling and Prediction of the Transmission Dynamics of COVID-19 Based on the SINDy-LM Method

**Yu-Xin Jiang**

Northwestern Polytechnical University

**Lin Du** (✉ [lindu@nwpu.edu.cn](mailto:lindu@nwpu.edu.cn))

Northwestern Polytechnical University <https://orcid.org/0000-0002-2749-5416>

**Xiong Xiong**

Northwestern Polytechnical University

**Shuo Zhang**

Northwestern Polytechnical University

**Jia-Xiang Wang**

Northwestern Polytechnical University

**Jia-Chun Li**

Northwestern Polytechnical University

---

## Research Article

**Keywords:** COVID-19, transmission dynamics, SINDy, data-driven, LM optimization algorithm

**Posted Date:** February 25th, 2021

**DOI:** <https://doi.org/10.21203/rs.3.rs-171097/v1>

**License:** © ⓘ This work is licensed under a Creative Commons Attribution 4.0 International License.

[Read Full License](#)

---

**Version of Record:** A version of this preprint was published at Nonlinear Dynamics on July 22nd, 2021.  
See the published version at <https://doi.org/10.1007/s11071-021-06707-6>.

# Modeling and Prediction of the Transmission Dynamics of COVID-19 Based on the SINDy-LM Method

Yu-Xin Jiang · Xiong Xiong ·  
Shuo Zhang · Jia-Xiang Wang ·  
Jia-Chun Li · Lin Du

Received: date / Accepted: date

**Abstract** The transmission dynamics of COVID-19 is investigated in this study. A SINDy-LM modeling method that can effectively balance model complexity and prediction accuracy is proposed based on data-driven technique. First, the Sparse Identification of Nonlinear Dynamical systems (SINDy) method is used to discover and describe the nonlinear functional relationship between the dynamic terms in the model in accordance with the observation data of the COVID-19 epidemic. Moreover, the Levenberg–Marquardt (LM) algorithm is utilized to optimize the obtained model for improving the accuracy of the SINDy algorithm. Second, the obtained model, which is consistent with the logistic model in mathematical form with small errors and high robustness, is leveraged to review the epidemic situation in China. Otherwise, the evolution of the epidemic in Australia and Egypt is predicted, which demonstrates that this method has universality for constructing the global COVID-19 model. The proposed model is also compared with the extreme learning machine (ELM), which shows that the prediction accuracy of the SINDy-LM method outperforms that of the ELM method and the generated model has higher sparsity.

**Keywords** COVID-19 · transmission dynamics · SINDy · data-driven · LM optimization algorithm

---

Y.-X. Jiang · X. Xiong · S. Zhang · J.-X. Wang · J.-C. Li · L. Du  
School of Mathematics and Statistics, Northwestern Polytechnical University, Xi'an, 710129, China  
E-mail: lindu@nwpu.edu.cn

S. Zhang · X. Xiong · L. Du  
MIIT Key Laboratory of Dynamics and Control of Complex Systems, 710129, China.

## 1 INTRODUCTION

At the beginning of 2020, Corona Virus Disease 2019 (COVID-19) occurred globally [2,3], and it is currently spreading worldwide on a large scale. Statistics from Johns Hopkins University in the United States showed that nearly 850,000 people have died of COVID-19 and more than 25,890,000 cases of infection have been confirmed in more than 180 countries and regions around the world as of September 31, 2020. The prediction of COVID-19 is an important task in the public health security. It can detect the development trend of the disease early and improve the predictability of the epidemic, which plays an important role in the prevention, treatment, and health decision making of the disease [4]. Therefore, the proposal of a universal prediction method for COVID-19 has important theoretical and practical significance for the guidance of epidemic prevention and control worldwide based on the development of the epidemic situation in China.

Model-driven and data-driven approaches are two main methods for the spread and prediction of COVID-19 at present. The traditional epidemiological models for studying infectious diseases consists of SIR and SEIR models [1]. Teles used the SIR model to simulate the MERS epidemic in Korea for assessing the evolution of the curve of the number of COVID-19 cases in Portugal [5]. Some researchers used the SEIR model to analyze and identify the transmission dynamics of the COVID-19. Huang et al. completed the prediction of the COVID-19 epidemic in some Asian countries based on the transmission dynamics and universal SEIR model [4]. Tang et al. derived the basic reproduction number of COVID-19 through SEIR model analysis [6]. Gaurav et al. employed the SEIR model and regression method to analyze and predict the development of the epidemic

in India [7]. Other researchers have also proposed some methods to improve and extend the SEIR model. He et al. used particle swarm algorithm to identify the parameters in the SEIR model and introduced seasonal and random infection parameters [8]. However, the above-mentioned references ignore that COVID-19 has a long incubation period and strong infectivity; these characteristics give rise to great difficulty in predicting specific parameters in the traditional model. If a high-dimensional complex model is established to reduce the difficulty of estimation, then some problems such as the inconsistency of the development trend of the state variables in the model with the actual data will be induced.

In addition to traditional epidemiological models, academic circles at home and abroad have proposed many research methods that use machine learning algorithms to predict the spread of COVID-19 [10]. Javid used the extreme learning machine (ELM) to make predictions [11], but some issues such as low prediction accuracy and poor model interpretability still exist. Although machine learning methods have the abovementioned shortcomings, models based on data-driven methods in machine learning have been widely employed in nearly every branch of engineering and applied mathematics [12, 13]. This framework serves as an alternative for the discovery of the dynamic equations for controlling the spread of infectious diseases. There have been some researchs that used data-driven methods to predict and analyze COVID-19 [14, 15, 16]. This data-driven method omits the complicated modeling process, which avoids the large error caused by parameter identification and has high practicability and universality [17, 18, 19]. Thus, it is often used in system identification [20]. However, data-driven modeling usually requires assumptions on the form of the model. Thus, the results are limited to linear dynamics, which can only produce valid results near the fixed point of dynamics [21]. In addition, if the data-driven method is used to establish a model to predict COVID-19, then it is also prone to problems such as over-fitting and low prediction accuracy in a long time. Therefore, designing a new data-driven method of the accurate prediction of the actual observation data of COVID-19, which could balance the complexity (interpretability) of the model of COVID-19 and the prediction accuracy, has become a key research topic and urgently needs a breakthrough at home and abroad.

The Sparse Identification of Nonlinear Dynamical systems (SINDy) method uses symbolic regression to discover and describe the nonlinear function of the relationship between variables and measured dynamic terms; this method also utilizes sparse representation to determine the correlation in an effective and scalable frame-

work model item [17, 18, 22]. This method has been used for feature selection and parameter identification of differential equations in physical models [19]. It can also effectively solve the problem that the number of hidden neurons in the construction of deep neural networks cannot be determined [20]. Adopting this method to establish a model of COVID-19 based on data-driven strategy can effectively avoid errors caused by infectious disease coefficients in the model of COVID-19; thus, a more accurate prediction result can be obtained. Moreover, this method has better interpretability than the other data-driven modeling methods. However, this data-driven method may have problems of overfitting and low prediction accuracy. Accordingly, appropriate and reasonable improvements are needed in order to derive a more stable optimization method.

Levenberg-Marquardt (LM) algorithm has the advantages of reducing the probability of falling into a local minimum value, strong stability, and fast convergence [23]. It has become a standard technique for solving nonlinear least square problems [24] and has been employed to optimize the learning process of neural networks [25]. However, the accuracy of the LM algorithm depends heavily on the selection of the initial value [23]. If the SINDy data-driven modeling is combined with the LM algorithm to optimize the parameters in the model, then the accuracy of the SINDy algorithm can be improved first. Second, it can also effectively overcome shortcoming of the LM algorithm that relies too much on the initial value. The combination of the two methods can achieve a more complete review of countries where the epidemic has ended and make more accurate predictions for countries where the epidemic has not ended. Thus, this combination can further solve the problems of determining the turning point of the epidemic.

This study presents a method that combines new data-driven methods with optimization algorithms the abovementioned discussion. The effect of balancing model complexity and interpretability simultaneously can be achieved by combining the SINDy method with the LM method. Focused on the transmission dynamics of infectious diseases, this study contributes to proposing a modeling method that can effectively balance interpretability and prediction accuracy based on a data-driven technique. The proposed modeling method could review the epidemic situation in Chinese mainland and predict the epidemic situation in other countries worldwide.

The paper is organized as follows. In Sect. 2, the basic principles of the nonlinear dynamic sparse recognition method and the LM algorithm are mainly introduced, and the “SINDy-LM” data-driven modeling

method that combines the two is proposed. In Sect. 3, the method is first applied to establish a COVID-19 model suitable for Chinese mainland. This section also judges the location of the “epidemic turning point” and the SINDy-LM method is applied to other countries in the world (Australia, Egypt). Sect. 4 discusses the robustness of the model and compares the SINDy-LM method with the ELM algorithm. The last section summarizes the conclusion and discusses the practical significance of the method, potential problems, and follow-up work.

## 2 Data-driven modeling based on SINDy-LM

In this section, the idea and algorithm procedure of SINDy method and LM algorithm are introduced in detail, and the two are combined to complete the establishment of the model.

### 2.1 Model setup based on SINDy method

The Sparse Identification of Nonlinear Dynamical systems (SINDy) method uses sparse regression and parameter identification to discover the reduced governing equations correctly from a large number of combined potential dynamic models. Steven L. Brunton and others introduced the background and partial applications of the SINDy method [17] and elaborated on using the SINDy method to study models and solve regression and selection problems [26].

This section introduces the SINDy method proposed by Steven L. Brunton [26]. The symbols used throughout the work are given as follows: lowercase letters (such as  $x$ ) represent scalars, and bold lowercase letters (such as  $\mathbf{x}$ ) represent vectors; bold uppercase letters (such as  $\mathbf{X}$ ) define matrices; parentheses emphasize functions and vector functions (such as  $f(\cdot)$ ); the relevance of variables with respect to time, such as  $x(t)$ , is emphasized when necessary.

SINDy method determines the governing equations in the infectious disease dynamics system by using the true observation data in many countries. The nonlinear dynamic system is expressed as Eq. (1):

$$\dot{\mathbf{x}}(t) = f(\mathbf{x}(t)), \quad (1)$$

where vector  $\mathbf{x}(t)$  represents the state of the system at time  $t$ ,  $\dot{\mathbf{x}}(t)$  represents the derivative of  $\mathbf{x}(t)$  at time  $t$ , and  $f(\mathbf{x}(t))$  is the evolution of  $\mathbf{x}(t)$  with time to represent constraints of the governing equation in the dynamic system. In the established COVID-19 model, the

main research goal is about the evolution of state variables such as the number of confirmed cases, deaths, cured cases and close contacts over time.

The specific form of the function  $f$  is determined by the observation data, and it requires collecting the time history of the state  $\mathbf{x}(t)$ . It needs to collect the COVID-19 time series data of  $\mathbf{x}(t)$  at  $t_1, t_2, \dots, t_m$  and construct the relevant numerical matrix Eqs. (2) and (3):

$$\mathbf{X} = \begin{bmatrix} \mathbf{x}^T(t_1) \\ \mathbf{x}^T(t_2) \\ \vdots \\ \mathbf{x}^T(t_m) \end{bmatrix} = \begin{bmatrix} x_1(t_1) & x_2(t_1) & \cdots & x_n(t_1) \\ x_1(t_2) & x_2(t_2) & \cdots & x_n(t_2) \\ \vdots & \vdots & \ddots & \vdots \\ x_1(t_m) & x_2(t_m) & \cdots & x_n(t_m) \end{bmatrix} \begin{matrix} \downarrow \text{time,} \\ \\ \\ \rightarrow \text{state} \end{matrix} \quad (2)$$

$$\dot{\mathbf{X}} = \begin{bmatrix} \dot{\mathbf{x}}^T(t_1) \\ \dot{\mathbf{x}}^T(t_2) \\ \vdots \\ \dot{\mathbf{x}}^T(t_m) \end{bmatrix} = \begin{bmatrix} \dot{x}_1(t_1) & \dot{x}_2(t_1) & \cdots & \dot{x}_n(t_1) \\ \dot{x}_1(t_2) & \dot{x}_2(t_2) & \cdots & \dot{x}_n(t_2) \\ \vdots & \vdots & \ddots & \vdots \\ \dot{x}_1(t_m) & \dot{x}_2(t_m) & \cdots & \dot{x}_n(t_m) \end{bmatrix}, \quad (3)$$

where  $\dot{\mathbf{X}}$  is approximated by the numerical differentiation of  $\mathbf{X}$ , and the data required in  $\mathbf{X}$  are the observation data collected from the measurement in the real world. In this study,  $x_1, x_2, \dots, x_n$  will be substituted into state variables such as the number of confirmed cases and the number of deaths.

A candidate function library  $\Theta(\mathbf{x})$  consisting of candidate nonlinear functions Eq. (4), where each column represents the potential candidate of the element in  $f(\cdot)$  to be discovered, is constructed. The function chosen to fill the library is arbitrary and can be composed of polynomial terms and trigonometric functions. The nonlinear feature library is leveraged to find the least dynamic term that satisfies Eq. (4); thus, a COVID-19 model is generated as follows:

$$\dot{\mathbf{X}} = \Theta(\mathbf{X})\Xi, \quad (4)$$

$$\Theta(\mathbf{X}) = \begin{bmatrix} | & | & | & | & \dots \\ \mathbf{1} & \mathbf{X} & \mathbf{X}^{P_2} & \mathbf{X}^{P_3} & \dots \\ | & | & | & | & \dots \end{bmatrix}, \quad (5)$$

where element  $\mathbf{1}$  represents a column vector composed of  $m$  ones, element  $\mathbf{X}$  is defined in Eq. (2), and element  $\mathbf{X}^{P_2}$  is the set of all quadratic polynomial functions of state vector  $\mathbf{x}$ .  $\mathbf{X}^{P_3}$  is the set of cubic polynomial functions. The superscript  $P_2$  is used to define the set

of quadratic polynomial functions with a structure as in Eq. (6):

$$\mathbf{X}^{P_2} = \begin{bmatrix} x_1^2(t_1) & x_1x_2(t_1) & \cdots & x_2^2(t_1) & \cdots & x_n^2(t_1) \\ x_1^2(t_2) & x_1x_2(t_2) & \cdots & x_2^2(t_2) & \cdots & x_n^2(t_2) \\ \vdots & \vdots & & \vdots & & \vdots \\ x_1^2(t_m) & x_1x_2(t_m) & \cdots & x_2^2(t_m) & \cdots & x_n^2(t_m) \end{bmatrix}. \quad (6)$$

Each column of  $\Theta(\mathbf{X})$  represents the candidate function term on the right side of the equation. A greater degree of freedom is obtained when selecting coefficients in this alternative function library. However, other dynamic systems such as infectious disease transmission systems usually have only a few nonlinear terms in practical applications. Thus, the right side of the equation has high sparsity in the high-dimensional nonlinear function space. As emphasized in the literature [26], the assumption that the algorithm can converge to the true solution is that only a few elements make up the function  $f(\cdot)$ ; this way makes it sparse in the space of possible functions [13]. This sparsity balances the complexity and accuracy of the model. In summary, a sparse regression problem can be established to determine the sparse vector of the coefficient matrix for obtaining the nonlinear effective function term. The objective function of SINDy is defined by  $\ell_1$  norm regression:

$$\xi_i = \arg \min_{\xi_i} \left\| \dot{\mathbf{X}} - \xi_i \Theta(\mathbf{X}) \right\|_2 + \lambda \left\| \xi_i \right\|_1, \quad (7)$$

where  $\xi_i$  collects the coefficients of candidate function  $\Theta(\mathbf{X})$ , which is the goal of minimization. The number of vectors is equal to the dimension  $n$  of the state vector with  $i = 1, \dots, n$ . Only a few candidate functions are expected to affect system dynamics; thus, all vectors are expected to be sparse. Symbols  $\|\cdot\|_1$  and  $\|\cdot\|_2$  represent  $\ell_1$  norm and  $\ell_2$  norm, respectively.  $\lambda$  is a scalar multiplier and element  $\lambda \left\| \xi_i \right\|_1$  is a regularization term that penalizes coefficients different from 0 in a linear manner. It is the real promoter of sparsity in the minimizing problem.

For Eq. (7), convex optimization algorithms such as least absolute shrinkage and selection operator (LASSO) can be used to solve. The method of sequential threshold least squares can also be used instead. The sequential threshold least square method applies sparsity by “manually” setting all coefficients less than  $\lambda$  to 0 in an iterative manner. The result is very similar to that produced by LASSO. For the sake of brevity, this study takes the latter solution.

After all the sparse vectors are estimated, they can be collected in the sparse matrix  $\Xi$ :

$$\Xi = \begin{bmatrix} | & | & | & \cdots & | \\ \xi_1 & \xi_2 & \cdots & \xi_n \\ | & | & | & \cdots & | \end{bmatrix}. \quad (8)$$

Given that  $\Xi$  is obtained, the model of each row of the control equation can be constructed as follows:

$$\frac{dx_i}{dt} = f_i(\mathbf{x}) = \Theta(\mathbf{x}^T) \xi_i, \quad (9)$$

where  $\mathbf{x} = (x_1, x_2, \dots, x_n)^T$ . Unlike the data matrix  $\Theta(\mathbf{X})$ ,  $\Theta(\mathbf{x}^T)$  is the sign function vector of element  $\mathbf{x}$ . In this way, a complete COVID-19 model is formed:

$$\dot{\mathbf{x}} = f(\mathbf{x}) = \Xi^T (\Theta(\mathbf{x}^T))^T. \quad (10)$$

According to Eq. (9), the governing equations followed by the components in the obtained COVID-19 model can be expressed as

$$\frac{dx_i}{dt} = b_{0,i} + b_{1,i}x_i + b_{2,i}x_i^2 + b_{3,i}x_i^3 + \cdots + b_{p,i}x_i^p, \quad (11)$$

where  $b_{0,i}, b_{1,i}, \dots, b_{p,i}$  are the elements of in the coefficient matrix  $\Xi = [\xi_1, \xi_2, \dots, \xi_n]$  with each  $\xi_i = (b_{0,i}, b_{1,i}, \dots, b_{p,i})^T$ .

## 2.2 Optimization of model coefficients with LM algorithm

The model generated by the SINDy method is more dependent on the selection of training data, and its advantage is that it has strong universality and flexibility. However, this data-driven method have problems with over-fitting and low prediction accuracy. Thus, appropriate and reasonable improvements are needed in order to derive a more stable optimization method.

The LM algorithm, which is a standard technique for solving nonlinear least square problems [23, 24], has been used to optimize the learning process of neural networks [25]. This study combines SINDy method with LM algorithm to optimize the parameters in the model.

According to the abovementioned SINDy method, Eq. (4) can be solved as Eq. (10), which is the specific coefficient matrix  $\Xi = [\xi_1, \xi_2, \dots, \xi_n]$  of the model. This study combines the SINDy method with the LM algorithm to iteratively optimize the items in  $\Xi$  for improving the accuracy of the coefficients  $\xi_i$  of each function in the model. As a result, better prediction results can be obtained.

The coefficients of each term in the model Eq. (11) directly obtained by the SINDy method are set as the

initial value of the iteration, which is set as  $\xi_i^{(0)}$ . Then, the principle of the iterative procedure is

$$\xi_i^{(k+1)} = \xi_i^{(k)} + \Delta \xi_i, \quad (12)$$

where  $\xi_i^{(k)}$  is the vector at the  $k$  iteration ( $k = 1, 2, \dots, M$ );  $\xi_i^{(k+1)}$  is the vector at the  $k + 1$  iteration;  $\Delta \xi_i$  is the variation during the two iterations. Next, assume that

$$\Delta \xi_i = - [\nabla^2 E(\xi_i)]^{-1} \nabla E(\xi_i), \quad (13)$$

$$E(\xi_i) = \frac{1}{2} \sum_{i=1}^M e_i^2(\xi_i), \quad (14)$$

where  $E(\xi_i)$  is the sum of squared error,  $\nabla E(\xi_i)$  is the gradient,  $\nabla^2 E(\xi_i)$  is the Hessian matrix of  $E(\xi_i)$ , and  $e_i(\xi_i)$  is the error, as shown in the following equations:

$$\nabla E(\xi_i) = \left[ \frac{\partial E}{\partial b_{0,i}} \quad \frac{\partial E}{\partial b_{1,i}} \quad \dots \quad \frac{\partial E}{\partial b_{p,i}} \right]^T, \quad (15)$$

$$\nabla^2 E(\xi_i) = \begin{bmatrix} \frac{\partial^2 E}{\partial b_{0,i}^2} & \frac{\partial^2 E}{\partial b_{0,i} \partial b_{1,i}} & \dots & \frac{\partial^2 E}{\partial b_{0,i} \partial b_{p,i}} \\ \frac{\partial^2 E}{\partial b_{1,i} \partial b_{0,i}} & \frac{\partial^2 E}{\partial b_{1,i}^2} & \dots & \frac{\partial^2 E}{\partial b_{1,i} \partial b_{p,i}} \\ \vdots & \vdots & \ddots & \vdots \\ \frac{\partial^2 E}{\partial b_{p,i} \partial b_{0,i}} & \frac{\partial^2 E}{\partial b_{p,i} \partial b_{1,i}} & \dots & \frac{\partial^2 E}{\partial b_{p,i}^2} \end{bmatrix}. \quad (16)$$

In the Gauss-Newton method, they are rewritten by

$$\nabla^2 E(\xi_i) \approx A^T(\xi_i) A(\xi_i), \quad (17)$$

$$\nabla^2 E(\xi_i) \approx A^T(\xi_i) A(\xi_i) + \mu I. \quad (18)$$

Among them,  $I$  is the identity matrix,  $\mu$  is the damping coefficient, and  $\mu > 0$  is a constant.  $A(\xi_i^{(k)})$  is the Jacobian matrix, as shown in the following equation:

$$A_k \triangleq A(\xi_i^{(k)}) = \begin{bmatrix} \frac{\partial e_1(\xi_i^{(k)})}{\partial b_{0,i}} & \frac{\partial e_1(\xi_i^{(k)})}{\partial b_{1,i}} & \dots & \frac{\partial e_1(\xi_i^{(k)})}{\partial b_{p,i}} \\ \frac{\partial e_2(\xi_i^{(k)})}{\partial b_{0,i}} & \frac{\partial e_2(\xi_i^{(k)})}{\partial b_{1,i}} & \dots & \frac{\partial e_2(\xi_i^{(k)})}{\partial b_{p,i}} \\ \vdots & \vdots & \ddots & \vdots \\ \frac{\partial e_M(\xi_i^{(k)})}{\partial b_{0,i}} & \frac{\partial e_M(\xi_i^{(k)})}{\partial b_{1,i}} & \dots & \frac{\partial e_M(\xi_i^{(k)})}{\partial b_{p,i}} \end{bmatrix}. \quad (19)$$

In summary, the expression of the LM algorithm is as Eq.(20) and (21):

$$\Delta \xi_i = - (A_k^T A_k + \mu I)^{-1} A_k^T e_k, \quad (20)$$

$$\xi_i^{(k+1)} = \xi_i^{(k)} - (A_k^T A_k + \mu I)^{-1} A_k^T e_k. \quad (21)$$

The error function value  $E(\xi_i^{(k)})$  needs to be recalculated and  $\mu_k$  needs to be set as the value of  $\mu$  in the  $k$  th iteration. Suppose  $\nu > 1$ , if  $E(\xi_i^{(k+1)}) < E(\xi_i^{(k)})$ , make  $\mu_{k+1} = \mu_k / \nu$  and stop decreasing  $\mu$  when  $E(\xi_i^{(k+1)}) > E(\xi_i^{(k)})$  is satisfied; if  $E(\xi_i^{(k+1)}) > E(\xi_i^{(k)})$ , make  $\mu_{k+1} = \mu_k \cdot \nu$  and stop updating  $\mu$  when  $E(\xi_i^{(k+1)}) < E(\xi_i^{(k)})$  is satisfied. Finally, the specific coefficient matrix  $\Xi^{(M)} = [\xi_1^{(M)}, \xi_2^{(M)}, \dots, \xi_n^{(M)}]$  after  $M$  iterations is obtained, as well as the optimized COVID-19 model.

### 3 MAIN RESULTS

#### 3.1 Review work in China

According to the infection cases in Chinese mainland reported by the National Health Commission of China, the cumulative number of confirmed cases, cumulative cures, cumulative deaths, and other epidemic data from February 25 to June 30, 2020 can be obtained.

On the basis of the proposed modeling method that combines the SINDy data-driven method and the LM optimization algorithm introduced above, 47 days of actual observation data from February 25, 2020 to April 1, 2020 are set as the training set. The data from April 2, 2020 to June 21, 2020 are used as the testing set to solve the COVID-19 model in Chinese mainland, which can realize the review and prediction of the epidemic.

By using the epidemic data from Chinese mainland, the coefficients of each function term at the right side of Eq. (10) are shown in Table 1.

**Table 1** Coefficients of each function item in the COVID-19 model

Function item	$x_i$	$x_i^2$
Confirmed cases	0.2204	$-2.6790e^{-6}$
Deaths	0.1715	$-5.6026e^{-5}$
Cured cases	0.2123	$-5.4154e^{-6}$
Close contacts	0.2122	$-3.3610e^{-7}$

Table 1 shows the coefficients of each function item at the right side of the governing equation followed by the cumulative number of confirmed cases, deaths, cured, and close contacts. The function items represented by the numbers on the horizontal axis are  $x$ ,  $x^2$ ,  $x^3$ , and  $x^{-1}$ . The coefficients of some function terms have been omitted in the table because they are all zero.

The results in Table 1 show that the coefficients of the dynamic terms in the COVID-19 model obtained using the SINDy-LM method have high sparsity, which is consistent with the underlying laws followed by other

infectious disease systems. It also demonstrates that the model obtained by this method has a certain interpretability compared with the model obtained by the general neural network algorithm.

Let  $N_c$  be the cumulative number of confirmed cases changing over time and  $N_d$  be the number of deaths. By substituting the data of the cumulative number of confirmed cases into Eq. (10), the specific expression of Eq. (11) is obtained by solving

$$\frac{dN_c}{dt} = b_{1,1}N_c + b_{2,1}N_c^2, \quad (22)$$

where  $b_{1,1} = 0.2391$ ,  $b_{2,1} = -3.0234e^{-6}$ .

Utilize the LM algorithm to iteratively optimize the coefficients, and obtain the optimized governing equation:

$$\frac{dN_c}{dt} = \hat{b}_{1,1}N_c + \hat{b}_{2,1}N_c^2, \quad (23)$$

where  $\hat{b}_{1,1} = 0.2204$ ,  $\hat{b}_{2,1} = -2.6790e^{-6}$ .

By solving Eq. (23), the analytical expression of the cumulative number of confirmed cases in the model can be obtained as Eq. (24):

$$N_c(t) = \frac{\alpha}{1 + e^{-\beta(t-\tau)}}, \quad (24)$$

where  $\alpha = 82269$ ,  $\beta = 0.2204$ ,  $\tau = 30.4959$ .

By comparing the Eq.(25) and the classic Logistic model [27],

$$N_c(t) = \frac{K}{1 + \left(\frac{K}{N_0} - 1\right) e^{-r(t-t_0)}}, \quad (25)$$

where  $K$  is the population capacity,  $N_0$  is the number of the population at time  $t_0$ , and  $r$  is the growth rate.

The mathematical form of Eq. (24) is exactly the same as that of Eq. (25). Thus, the mathematical model followed by the cumulative number of confirmed cases is the logistic model with  $K = 82269$ ,  $r = 0.2204$ . The Chinese government employed effective anti-epidemic policies after the outbreak. Thus, it strictly controlled the number of people entering and leaving the country. Therefore, Chinese mainland can be regarded as a unit, in which the vast majority of cases occurred without any major ‘‘import’’ or ‘‘export’’ events. Therefore, the logistic model is indeed suitable for the prediction and analysis of the development of the epidemic in Chinese mainland.

The governing equation for the cumulative number of deaths in the COVID-19 model constructed with the SINDy-LM method is as shown in Eq. (26),

$$\frac{dN_d}{dt} = \hat{b}_{1,2}N_d + \hat{b}_{2,2}N_d^2, \quad (26)$$

where  $\hat{b}_{1,2} = 0.1715$ ,  $\hat{b}_{2,2} = -5.6026e^{-5}$ .

The previous analysis shows that the cumulative number of deaths in China is also consistent with the logistic model, with model parameters  $K = 3061.3104$ ,  $r = 0.1715$ . Therefore, the COVID-19 model obtained is compatible with the traditional epidemiological model and conforms to the natural law followed by the infectious disease transmission dynamic system.

Compared with the prediction results that directly uses the logistic model and identifies the parameters, the SINDy-LM method simplifies the process of analyzing many assumptions and is obviously more concise and powerful. Compared with other machine learning algorithms such as deep neural networks, SINDy-LM also avoids problems such as the uncertainty of neurons in the hidden layer. The resulting model is more interpretable.

According to the differential equations (such as Eqs. (23) and (26)) followed to obtain the state variables, the results of the review and prediction of the cumulative number of confirmed cases and deaths in Chinese mainland are shown in Fig. 1. The goodness of fit  $R^2$  is greater than 0.95, which confirms that the model generated by the SINDy-LM method has high accuracy. Moreover, the curve trend of the cumulative number of confirmed cases and deaths obtained is consistent with the actual trend. The relative error is also within the controllable range.

As shown in Fig. 1, the left side of the black dotted line represents the training set data, and the right side represents the testing set data. The blue solid line is the true data, and the red dotted line is the predicted data.

### 3.2 Forecasting work of the other country

In addition to China, this section also predicts and analyzes the evolution of the epidemic situation in other countries to verify whether this method is universal in other areas of the world. From the ‘‘Baidu Pandemic Real-time Big Data Report’’ website, relevant epidemic data in Australia and Egypt can be obtained during the 180 days after the outbreak. Based on the SINDy-LM method introduced above, the COVID-19 model is established and solved with the observation data.

The coefficients of the dynamic terms in Eq. (23) of the COVID-19 model followed in Australia are

$$\hat{b}_{1,1} = 0.1637, \hat{b}_{2,1} = -5.0489e^{-5}.$$

The figure of the cumulative number of confirmed cases changing over time is shown in Fig. 3.

The prediction of the number of cumulative cases in Australia can be obtained using the SINDy-LM method.

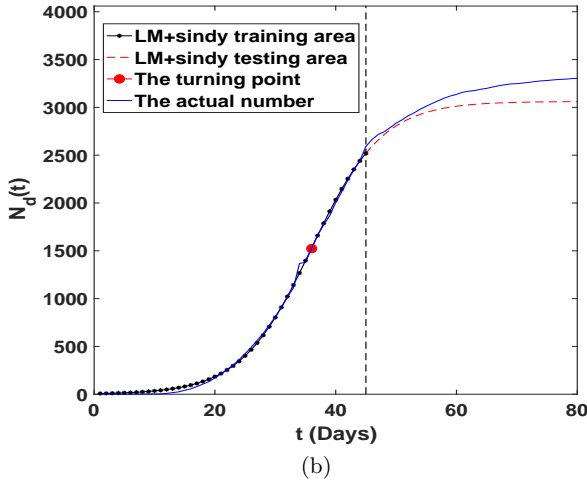
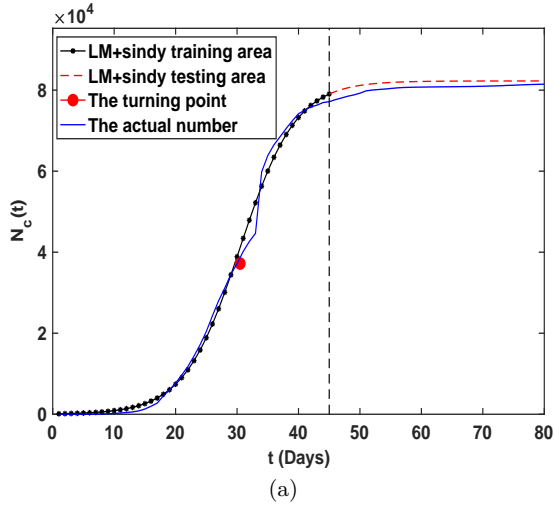


**Fig. 1** Review results of Chinese mainland in the COVID-19 model followed by (a) the cumulative number of confirmed cases and (b) the cumulative number of deaths

The red dotted line in Fig. 3 represents the prediction result, the blue realization represents the actual data, the black dotted line is the training set, and the right part is the testing set. Fig. 3 shows that the results using this method are consistent with the actual results on the testing set. The trend of the curve is also roughly the same as the actual curve trend, and the goodness of fit  $R^2$  is 0.99926. The relative error of the prediction is small, and the accuracy of the model is high. Similarly, the dynamic coefficients of the cumulative number of confirmed cases in Egypt in Eq. (23) are

$$\hat{b}_{1,1} = 0.0627, \hat{b}_{2,1} = -6.3115e^{-7}.$$

Fig. 4 shows the review and prediction of the epidemic in Egypt. The results are in line with the true situation. The goodness of fit is  $R^2 = 0.99959$ , which

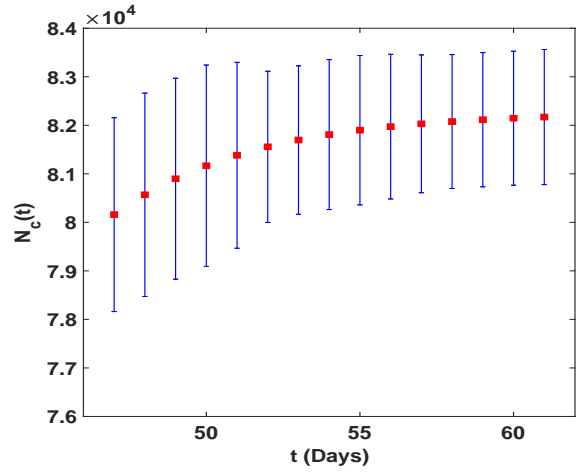


**Fig. 2** Error bar graph obtained by predicting the cumulative number of confirmed cases in the next 15 days

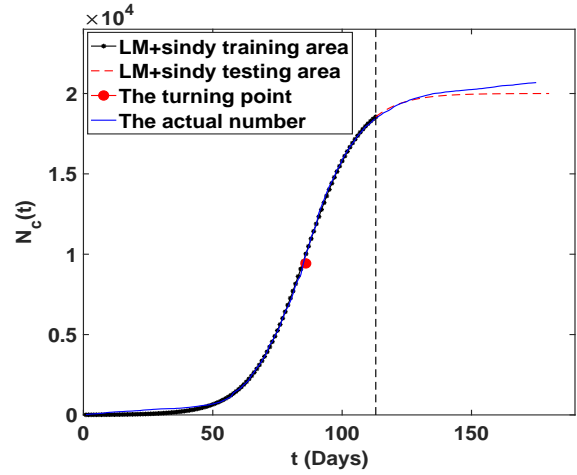


**Fig. 3** Prediction results of Australia in the COVID-19 model (the number of cumulative cases)

shows that the relative error of the prediction results is also within the controllable range.

The prediction of the COVID-19 epidemic in Australia and Egypt shows that the SINDy-LM method can make accurate review and high-precision predictions on the development of the epidemic in other countries. The prediction of the epidemic has some universality.

### 3.3 Exploring the “epidemic turning point”

According to the foregoing, the cumulative number of confirmed cases in the dynamics of COVID-19 transmission with the SINDy-LM follows the logistic model, as shown in Eq. (24). The logistic model follows the “S-curve”. To find epidemic turning point of the S-curve, it implies

$$N'_c(t) = \frac{r}{K} N_c(t)(K - N_c(t)), \quad (27)$$

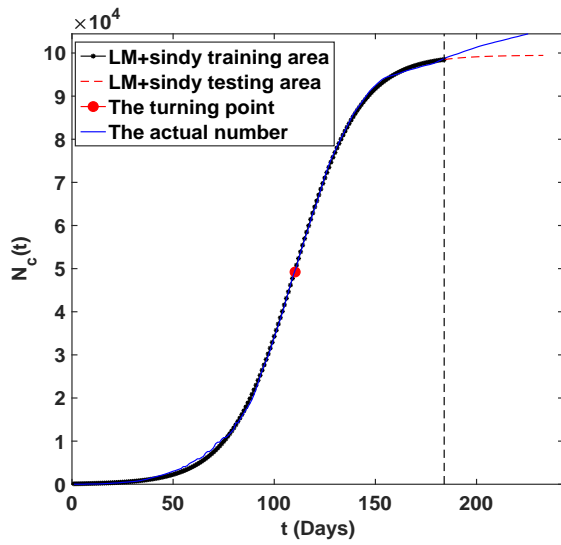


Fig. 4 Prediction of Egypt in the COVID-19 model (the number of cumulative cases)

$$\begin{aligned} N_c''(t) &= \frac{r}{K} N_c'(t)(K - N_c(t)) - \frac{r}{K} N_c(t) N_c'(t) \\ &= \left(\frac{r}{K}\right)^2 N_c(t)(K - N_c(t))(K - 2N_c(t)). \end{aligned} \quad (28)$$

Because  $N_c''(t) = 0$  and  $0 < N_c(t) < K$ , the turning point should occur at the time when  $N_c(t) = \frac{K}{2}$ .

The “epidemic turning point” can be predicted from the abovementioned model. When 45 days of data are used as the training set, the turning point can be obtained at the time when  $N_c(t) = \frac{K}{2} = 41134 - 41135$ , which is around the 31st day from January 10, 2020. The turning point is February 9, 2020. Compared with true data, it shows that the actual turning point is February 11, 2020. Considering that the model has a certain time lag, this model is more accurate in predicting the turning point of the epidemic in Chinese mainland.

The red dot in Fig. 5 is the turning point in Chinese mainland as determined in this study, that is, the “epidemic turning point,” which occurs at the time when  $N_c(t) = \frac{K}{2}$ . Fig. 5(a) represents the result using 45-day data as the turning point of the epidemic situation determined by the training set. Fig. 5(b) represents the result using 35-day data as the turning point of the epidemic situation determined by the training set.

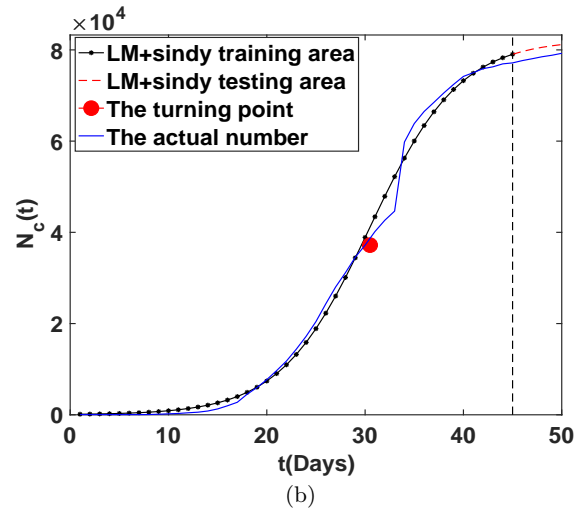
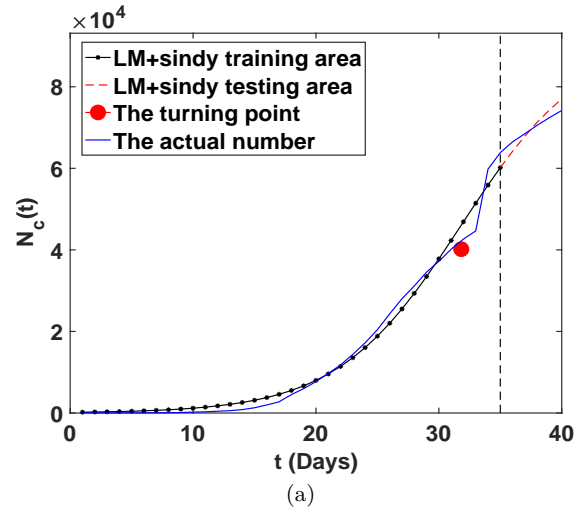


Fig. 5 Epidemic turning point in the COVID-19 model of cumulative cases in Chinese mainland followed by (a) the results using 35-days data and (b) the results using 45-days data

## 4 DISCUSSION

### 4.1 Robustness analysis

We choose actual observation data in different time periods as the training set to verify the robustness of the model, and we observe its fitting effect again. In this study, the goodness of fit is used to measure the degree of agreement between the model and the actual observation data. The statistic for measuring the goodness of fit is the coefficient of determination  $R^2$ , which is defined as Eq. (29):

$$R^2 = 1 - \frac{\sum_{i=1}^n [y_i - \bar{y}]^2}{\sum_{i=1}^n [f(t_i) - y_i]^2}. \quad (29)$$

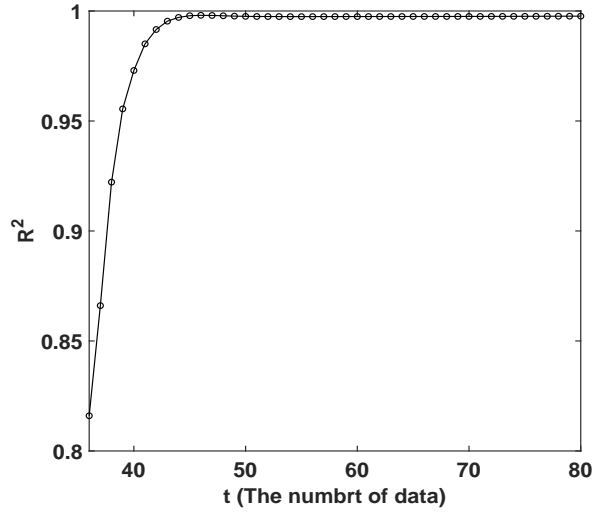
In Eqs.(29) and (30),  $f(t_i)$  represents the fitted value, and  $y_i$  represents the observed value. According to the definition of Eq. (29), the model fits the observations better when  $R^2$  is closer to 1. On the contrary, the fit is worse and the model is unreliable when the value of  $R^2$  is smaller. Observational data reveals that the cumulative number of confirmed cases in Chinese mainland reached the highest peak in a single day on February 11, 2020. The reason is that the government changed the detection standards, which caused a surge in the number of infection cases that day, thereby causing an abnormality. To avoid such anomalous data interference, we select the true observation data from February 15, 2020 to April 1, 2020 as the original training set. The data from April 2, 2020 to June 21, 2020 are used as the initial testing set. The SINDy-LM method is used to establish a COVID-19 model, and a function graph with the coefficient of determination varying with the amount of data used in the training set is obtained as shown in Fig. 6(a). According to Fig. 6(a), the coefficient of determination  $R^2$  shows an increasing trend with the amount of data used in the first 40 days. This result is due to the lack of data in the previous period and the unstable model. However,  $R^2$  has exceeded 0.95 after using 40 days of data. The fluctuation range has shrunk, and it has remained stable in an infinitely close range. The model has been very stable and robust after the testing set data volume exceeds 40 days. This result implies that the SINDy-LM method only needs to utilize limited data to build a COVID-19 model with high prediction accuracy. This property has a very positive effect on the prediction and control of the middle and late stages of the epidemic.

In addition to the goodness of fit, the mean squared error (MSE) is often regarded as an important indicator to measure the prediction results in practical applications. MSE represents the average of the sum of squares of the difference between the predicted and true values, and its mathematical expression is

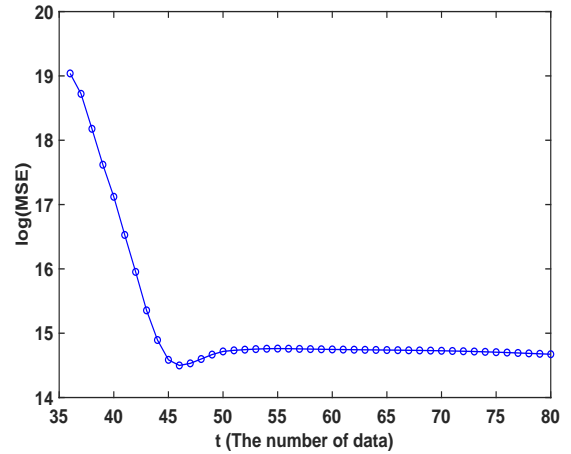
$$\text{MSE} = \frac{1}{n} \sum_{i=1}^n [f(t_i) - y_i]^2. \quad (30)$$

Given Eq. (30), MSE is not fixed. It will have a certain change depending on the selected data changes. We make a chart of MSE with the variation in amount of data used and also study the changes of accuracy in the model.

Fig. 6(b) is a figure of the mean square error with the amount of data used. The mean square error shows a decreasing trend as the amount of data increases in the first 35 days. This result is due to the lack of data in the previous period and the low degree of model fit and accuracy. As the amount of data increases, the model



(a)



(b)

**Fig. 6** Robustness analysis of the model followed by (a) variation in goodness of fit ( $R^2$ ) with the amount of data used and (b) the variation of mean square error (MSE) with the amount of data used

tends to stabilize, and the degree of fit and accuracy are significantly improved. After using 46 days of data, the mean square error increases slightly. This increase is due to that the base number of confirmed cases has reached a large value after 45 days, and the mean square error is slowly increasing because of its influence. After using 53 days of data, the mean square error has reached a relatively small value, and it begins to decline slowly. The accuracy of the model also continues to improve.

#### 4.2 Comparison with other methods (ELM algorithm)

In the prediction of the COVID-19 epidemic, many institutions use machine learning methods except ana-

lytical modeling methods to build prediction models for COVID-19. Among them, Johns Hopkins University used the method of ELM [11]. The ELM is a learning algorithm based on single hidden layer feedforward neural networks (SLFNs), which can omit complex analysis and modeling procedure and simplify calculations. However, when the original data are mixed with a large number of noise variables, the classification and regression accuracy of the ELM algorithm are greatly reduced, and the robustness of the obtained model is poor. In addition, this neural network-based machine learning algorithm cannot produce a model with interpretability.

To further explore the advantages of the SINDy-LM method compared with machine learning algorithms, this study compares the two methods by reviewing and predicting the epidemic in China.

First, the data of the first 40 days of the epidemic in China are taken as the training set, and the data of the last 40 days as the testing set. The activation function in SLFNs is composed of elementary function libraries, which must be infinitely differentiable. The input weights and hidden layer deviations of SLFNs can be randomly assigned according to the relevant theory of ELMs. Therefore, SLFNs can be simply considered a linear system. We can analytically calculate the output weights connecting the hidden and output layers through simple generalized inverse operations of the hidden layer output matrix to determine the structure of SLFNs and give the prediction results. The review and prediction results of the epidemic situation in Chinese mainland by using the ELM method are shown in Fig. 7.

In Fig. 7, the results in (a) are obtained using the ELM method to obtain the review and prediction results of the cumulative number of confirmed cases in China; those in (b) are obtained using the ELM method to obtain the review and prediction results of the cumulative number of deaths in China. The red dotted line represents the prediction result, the blue solid line represents the true data, the left side of the black dotted line is the training set, and the right side is the testing set. The red dotted line represents the prediction result, the blue solid line represents the actual data, the left side of the black dotted line is the training set, and the right side is the test set.

According to the results in Fig. 7, the gap between the predicted results obtained using the ELM method and the actual results becomes very large when predicting the cumulative number of confirmed cases and cumulative number of deaths in China in the next 40 days. Moreover, the development of the cumulative number of confirmed cases and deaths does not match the facts.

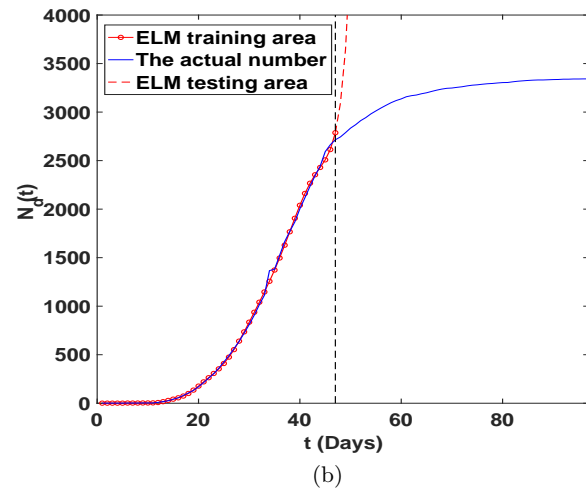
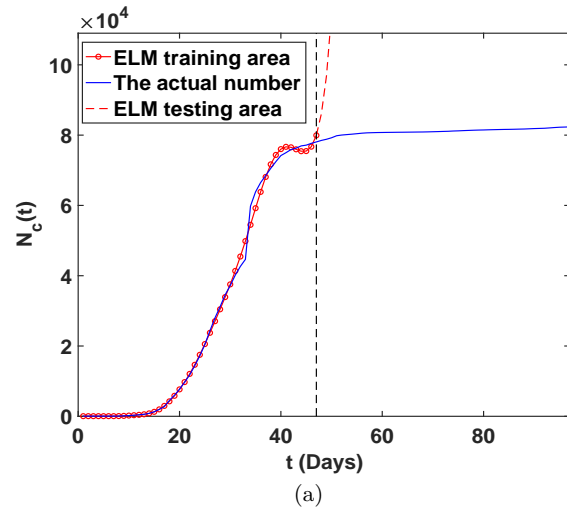


**Fig. 7** Reconsideration results of Chinese mainland using ELM method followed by (a) the cumulative number of confirmed cases and (b) the cumulative number of deaths

Similar results are obtained after changing the amount of data in the training set, which shows that the robustness of the model is very bad. The relative error produced by the short-term prediction is quantified and compared.

**Table 2** Relative error of the SINDy-LM method and ELM method

Forecast days	1 day	3 days	5 days	7 days
SINDy-LM	0.0156	0.041	0.079	0.123
ELM	0.551	0.721	0.891	0.919

Table 2 and Fig. 8 show that the prediction accuracy obtained by SINDy-LM method in epidemic prediction outperforms that of the ELM method. However,

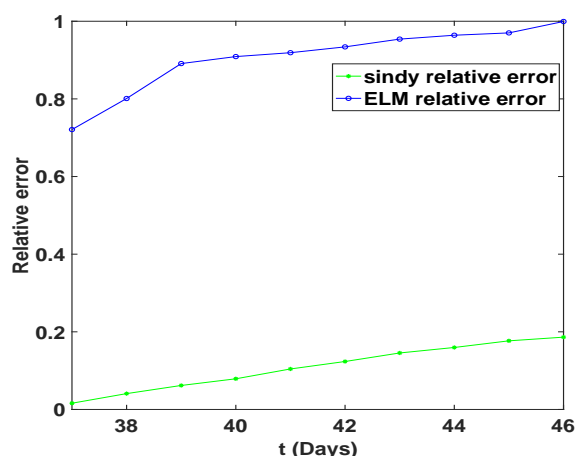


**Fig. 8** Relative error of the ELM and SINDy-LM methods varies with time

it will also accumulate quickly, and large errors and instabilities will occur when making long-term predictions. Thus, the accuracy and robustness of the model are poor. To be brief, the relative error obtained by the SINDy-LM method is smaller, and it is more stable over time. Therefore, the obtained model has better accuracy and robustness.

## 5 CONCLUSION

In this study, a SINDy-LM method is proposed to model and study the COVID-19 transmission system, which balances complexity and prediction accuracy simultaneously. First, the prediction results of this method in Chinese mainland, Australia, and Egypt are given, which indicate high accuracy and a certain universality of the derived method. Especially, the studied model accurately determines that the “the epidemic turning point” in China will appear on February 9, 2020. Second, the COVID-19 model produced by this method has strong sparsity, and the result has less fluctuation with the amount of data used. Finally, comparing the “SINDy-LM” and ELM methods, it can be demonstrated that the former is better than the latter in terms of model interpretability and prediction accuracy, which plays an important role in providing action guidelines to do a good job in epidemic prevention and control under normal conditions.

This study only considers one dimension when using the SINDy-LM method for modeling and forecasting. In the future, we will consider using SINDy-LM method to solve high-dimension problems. We will also attempt to apply the SINDy-LM algorithm to the parameter identification in the traditional analytical modeling to solve the problem of difficult parameter identification

in classical analytical modeling in order to make up for the poor interpretability of data-driven modeling at the same time.

**Acknowledgements** This work was supported by the National Natural Science Foundation of China (Nos. 11972292, 11902252, 11672233), the foundation of National Key Laboratory of Science and Technology on Aero-dynamic Design and Research (No. 614220119040101) and the National Training Program of Innovation and Entrepreneurship for Undergraduates (No. S202010699139). The authors also thanks Jiumei He and Hao Yuan for their discussion.

## Conflict of interest

The authors declare that they have no conflict of interest.

## References

1. Kermack, W.O., McKendrick, A.G.: A contribution to the mathematical theory of epidemics. Proceedings of the royal society of london. Series A, Containing papers of a mathematical and physical character, 115(772): 700-721 (1927)
2. Anderson, R.M., May, R.M.: Population biology of infectious diseases: Part I. Nature. 280(5721), 361-367 (1979)
3. Coronavirus: Common symptoms, preventive measures, and how to diagnose it. Caringly Yours [Online]. Available: <https://www.caringlyyours.com/content/2020/01/28> (2020)
4. Huang, S.Z., Peng, Z.X., Jin, Z.: Research on Novel Coronavirus Pneumonia Epidemic Control Strategy: Efficiency Evaluation and Recommendations. Science in China: Mathematics. 50(06), 885-898 (2020)
5. Teles, P.: Predicting the evolution of Covid-19 in Portugal using an adapted SIR model previously used in South Korea for the MERS outbreak. medRxiv [Online]. Available: <https://www.medrxiv.org/content/early/2020/03/25/2020.03.18.20038612> (2020)
6. Tang, B., Wang, X., Li, Q., et al.: Estimation of the Transmission Risk of 2019-nCoV and Its Implication for Public Health Interventions. Journal of Clinical Medicine. 9(2), 462 (2020)
7. Gaurav, P., Poonam, C., Rajan, G., et al.: SEIR and Regression Model based COVID-19 outbreak predictions in India. arXiv preprint arXiv: 2004.00958 (2020)
8. He, S., Peng, Y., Sun, K.: SEIR modeling of the COVID-19 and its dynamics. Nonlinear Dynamics. 101(3), 1667-1680 (2020)
9. Hou, C., Chen, J., Zhou, Y., et al.: The effectiveness of quarantine of Wuhan city against the Corona Virus Disease 2019 (COVID-19): A well-mixed SEIR model analysis. Journal of Medical Virology. 92(7), 841-848 (2020)
10. Yang, Z., Zeng, Z., Wang, K., et al.: Modified SEIR and AI prediction of the epidemics trend of COVID-19 in China under public health interventions. Journal of Thoracic Disease. 12(3), 165 (2020)
11. Javid, A.M., Liang, X., Venkitaraman, A., et al.: Predictive Analysis of COVID-19 Time-series Data from Johns Hopkins University. arXiv preprint arXiv:2005.05060 (2020)
12. Loiseau, J.C., Brunton, S.L.: Constrained sparse Galerkin regression. arXiv preprint arXiv:1611.03271 (2016)

13. Schaeffer, H.: Learning partial differential equations via data discovery and sparse optimization. *Proceedings of the Royal Society A: Mathematical, Physical and Engineering Sciences*. 473(2197), 1364-5021 (2017)
14. Huang, N.E., Qiao, F., Tung, K.K.: A data-driven tool for tracking and predicting the course of COVID-19 epidemic as it evolves. medRxiv [Online]. Available: [https://www.medrxiv.org/content/early/2020/05/23/2020.03.28.20046177\(2020\)](https://www.medrxiv.org/content/early/2020/05/23/2020.03.28.20046177(2020))
15. Hermanowicz, S.W.: Simple model for Covid-19 epidemics-back-casting in China and forecasting in the US. medRxiv [Online]. Available: [https://www.medrxiv.org/content/2020/04/03/2020.03.31.20049486\(2020\)](https://www.medrxiv.org/content/2020/04/03/2020.03.31.20049486(2020))
16. Huang, N.E., Qiao, F.: A data driven time-dependent transmission rate for tracking an epidemic: a case study of 2019-nCoV. *ence Bulletin*. 65(6), 425-427 (2020)
17. Brunton, S.L., Proctor, J.L., Kutz, J.N.: Discovering governing equations from data by sparse identification of nonlinear dynamical systems. *Proceedings of the National Academy of Sciences*, 113(15), 3932-3937 (2016)
18. Mangan, N.M., Kutz, J.N., Brunton, S.L., et al.: Model selection for dynamical systems via sparse regression and information criteria. *Proceedings Mathematical Physical and Engineering Sciences*. 473(2204), 1364-5021 (2017)
19. Corbetta, M.: Application of sparse identification of nonlinear dynamics for physics-informed learning. 2020 IEEE Aerospace Conference. IEEE, 1-8 (2020)
20. Ljung, L.: *System identification: theory for the user*. Tsinghua University Press, Tsinghua (2002)
21. Suhubi, E.S.: *Nonlinear oscillations, dynamical systems, and bifurcations of vector fields: Applied Mathematical Science*, Vol. 42, J. Guckenheimer and P. Holmes, Springer-Verlag, New York, Berlin, Heidelberg, Tokyo (1983). XVI + 453 pp. 206 figs, DM 104. *International Journal of Engineering Science*. 26(2), 221-222 (1988)
22. Schmidt, M., Lipson, H.: Distilling free-form natural laws from experimental data. *science*. 324(5923), 81-85 (2009)
23. Wang, B.X.: *Research on LM optimization algorithm and neural network predictive control in nonlinear systems*. Taiyuan University of Technology Press, Taiyuan (2016)
24. Lourakis, M.I.A.: A brief description of the Levenberg-Marquardt algorithm implemented by levmar. *Foundation of Research and Technology*. 4(1), 1-6 (2005)
25. Wilamowski, B.M., Yu, H.: Improved Computation for Levenberg-Marquardt Training. *IEEE Transactions on Neural Networks*. 21(6), 930-7 (2010)
26. Brunton, S.L., Kutz, J.N.: *Data-Driven Science and Engineering: Machine Learning, Dynamical Systems, and Control*. (2019)
27. Wu, K., Darcet, D., Wang, Q., et al.: Generalized logistic growth modeling of the COVID-19 outbreak in 29 provinces in China and in the rest of the world. arXiv preprint arXiv:2003.05681 (2020)

# Figures

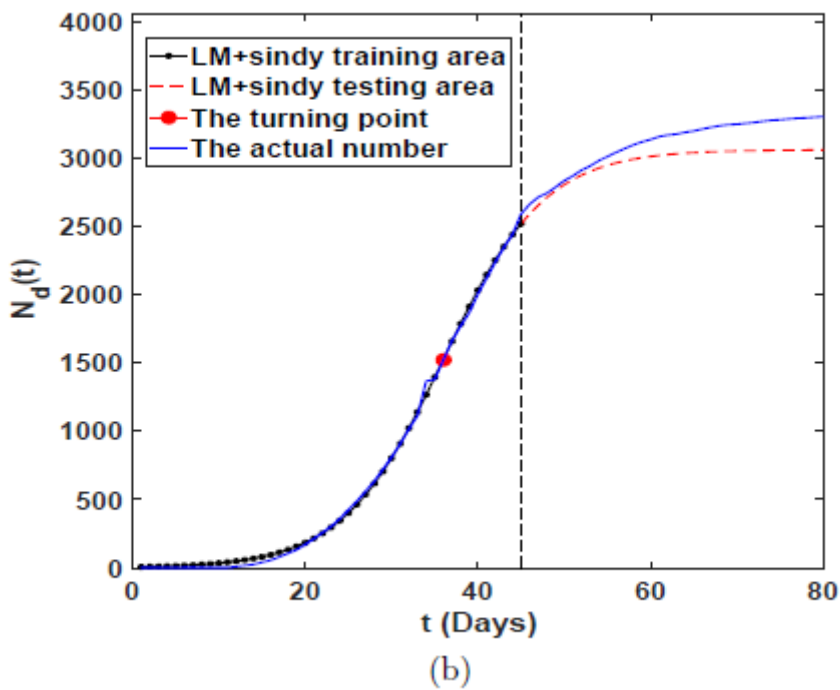
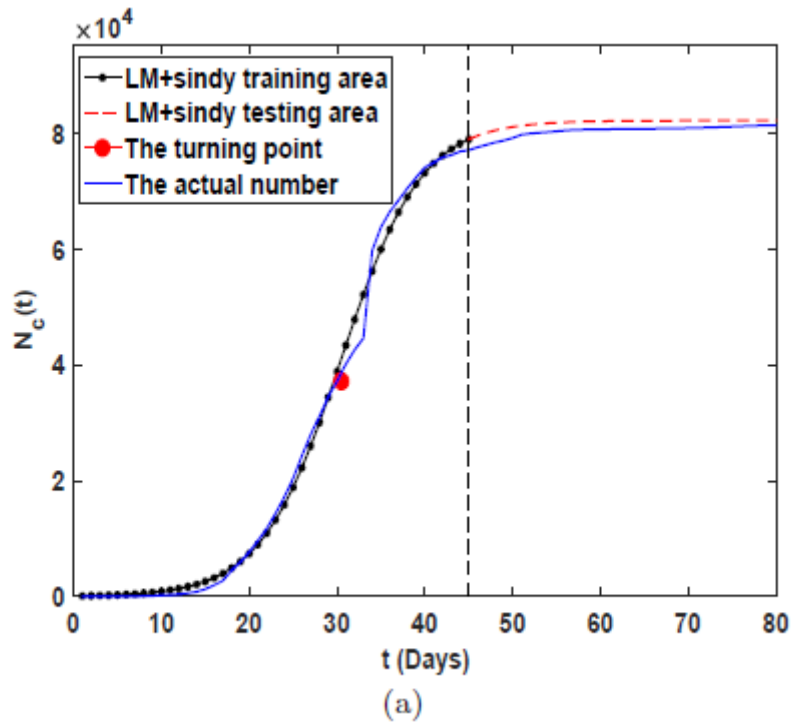


Figure 1

Review results of Chinese mainland in the COVID-19 model followed by (a) the cumulative number of confirmed cases and (b) the cumulative number of deaths

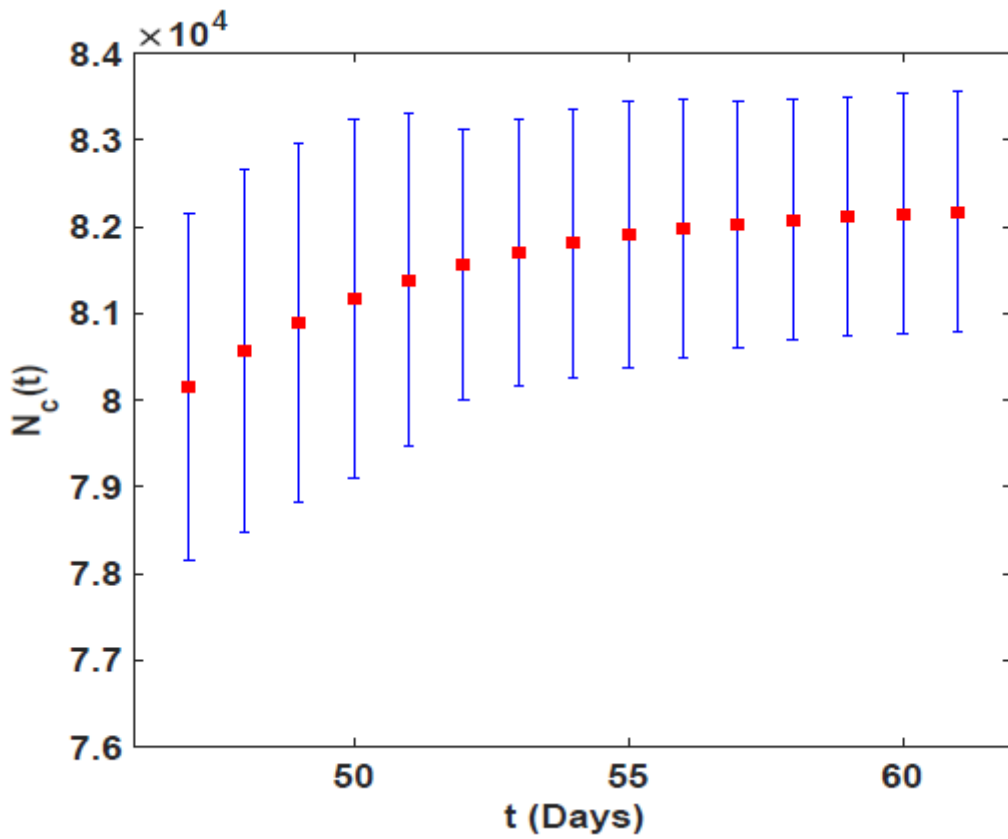


Figure 2

Error bar graph obtained by predicting the cumulative number of confirmed cases in the next 15 days

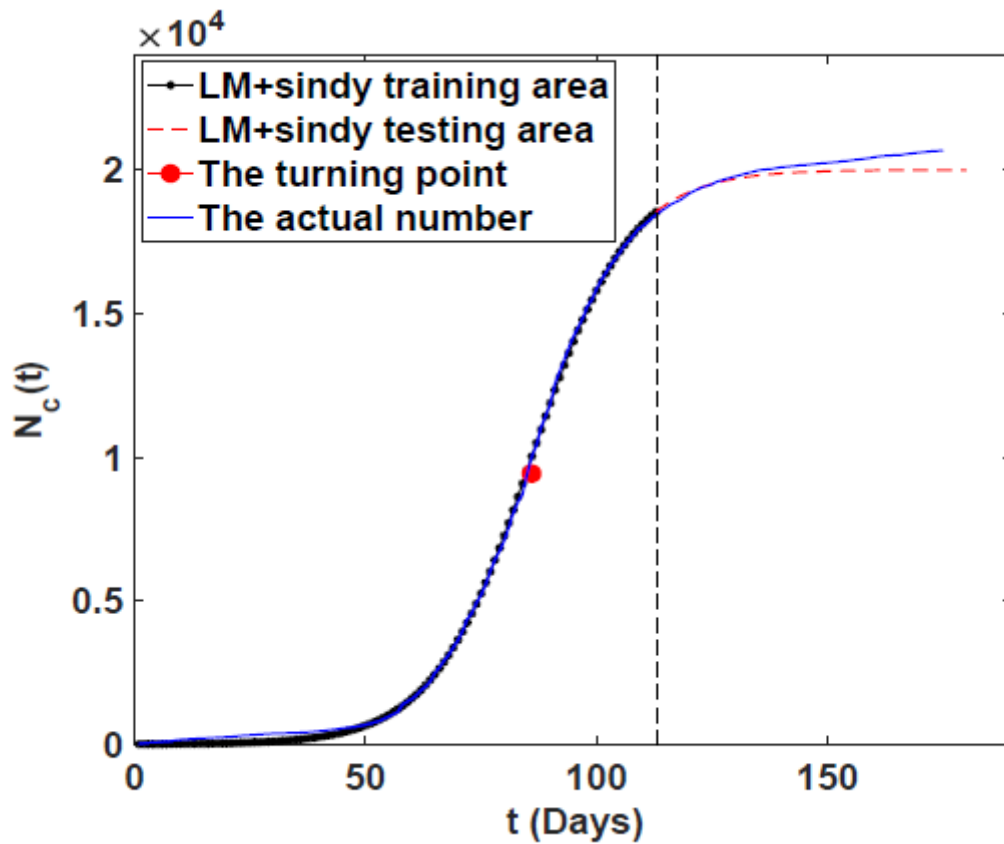


Figure 3

Prediction results of Australia in the COVID-19 model (the number of cumulative cases)

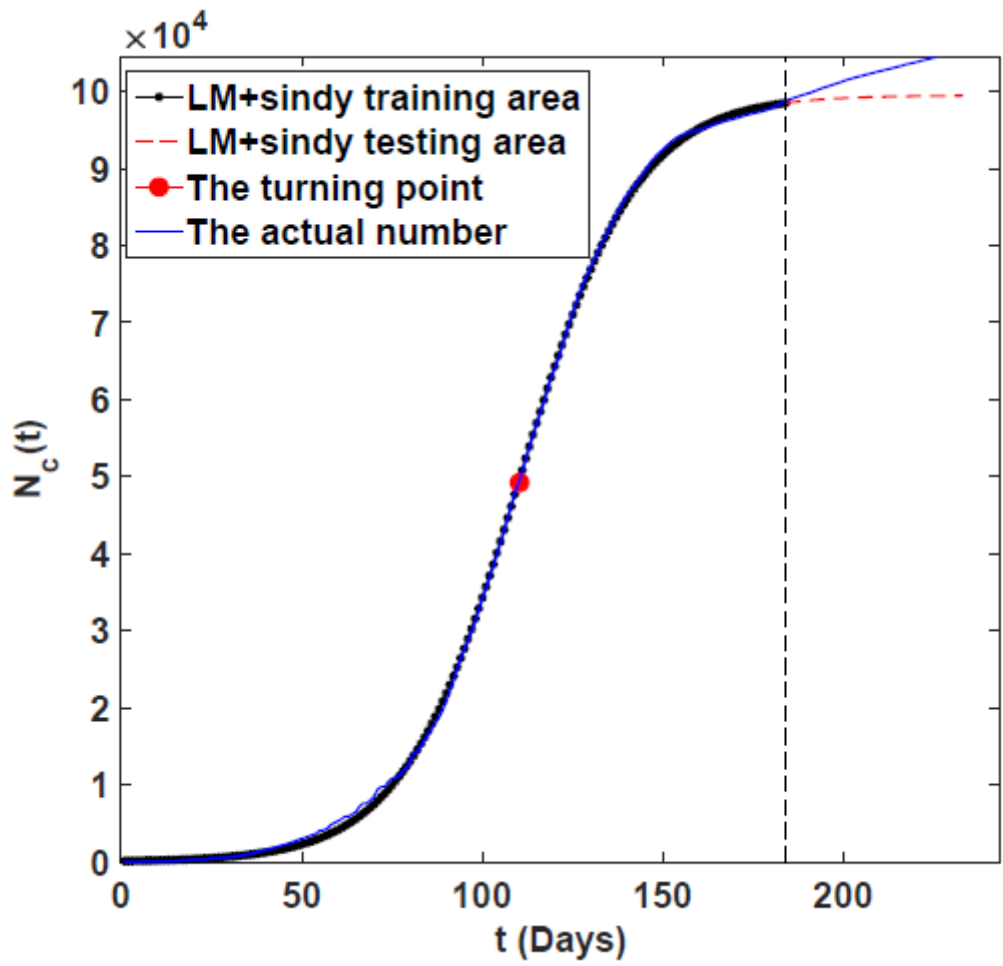
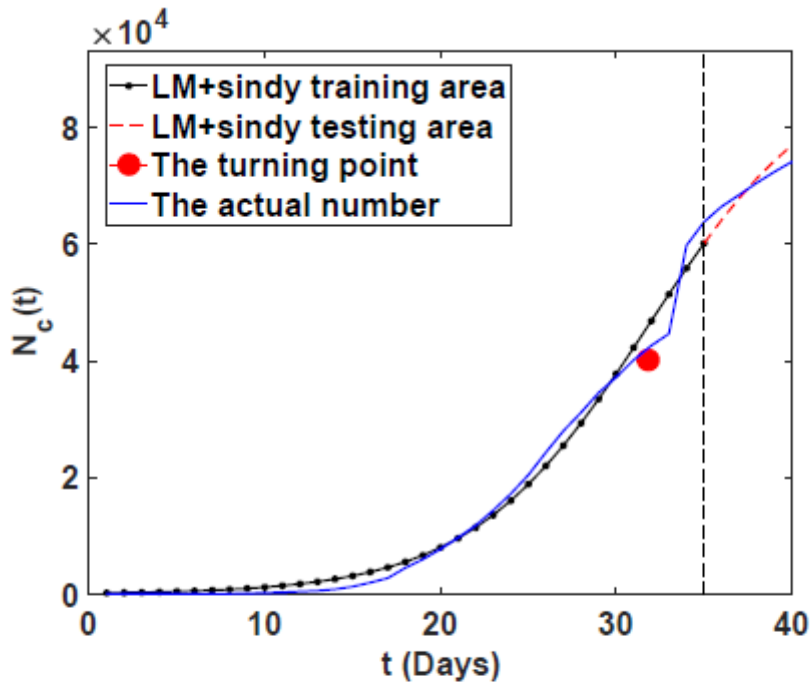
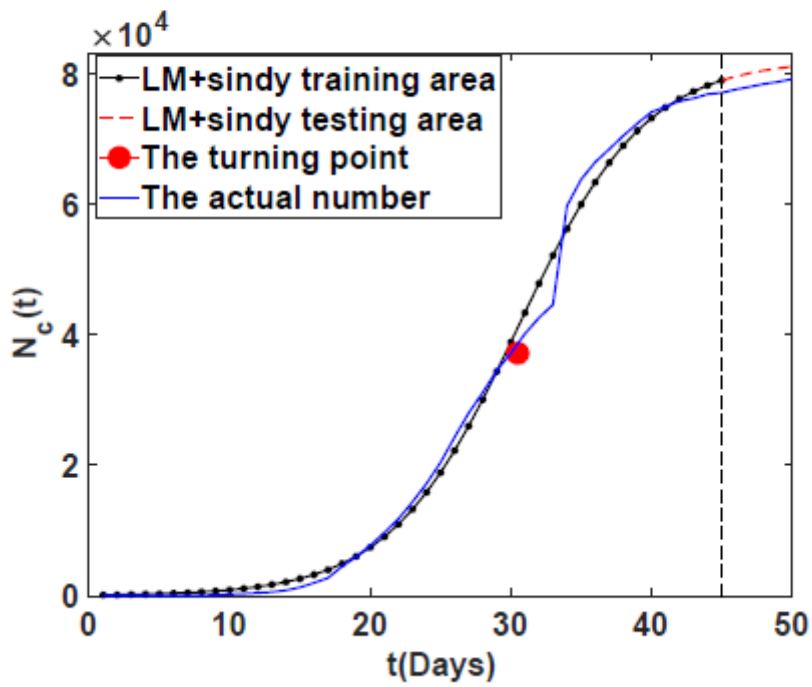


Figure 4

Prediction of Egypt in the COVID-19 model (the number of cumulative cases)



(a)



(b)

Figure 5

Epidemic turning point in the COVID-19 model of cumulative cases in Chinese mainland followed by (a) the results using 35-days data and (b) the results using 45-days data

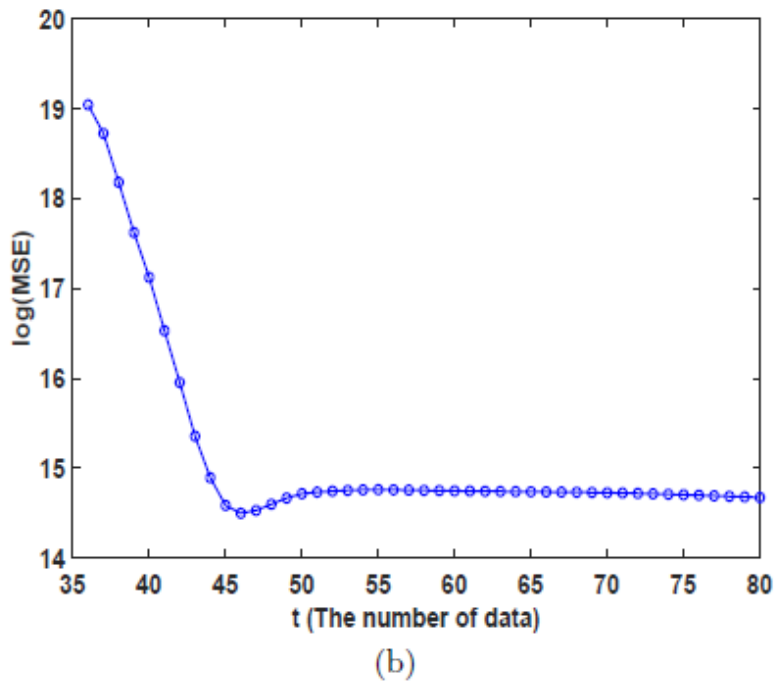
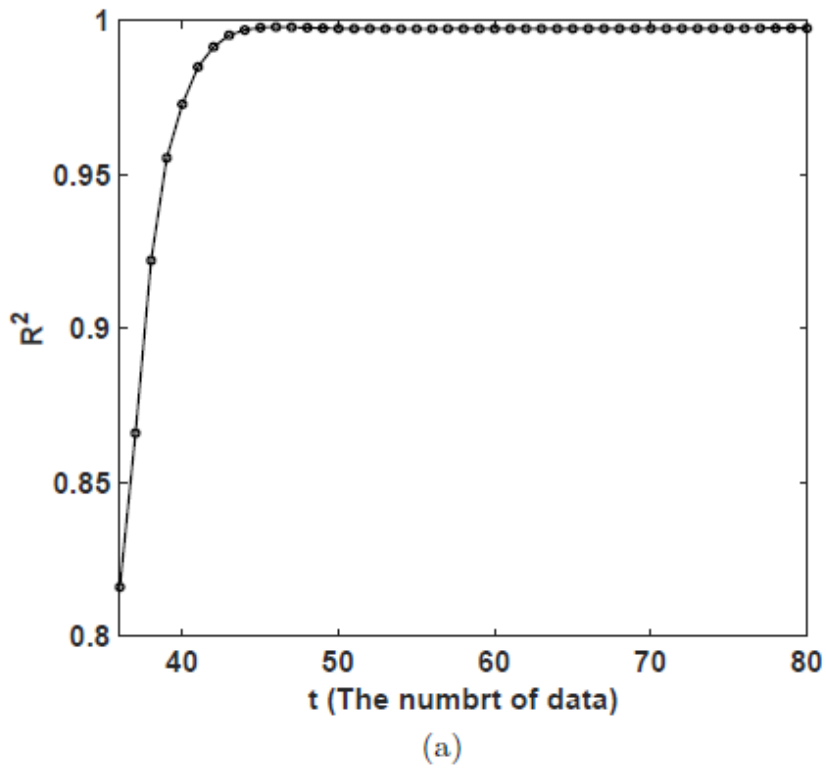


Figure 6

Robustness analysis of the model followed by (a) variation in goodness of fit ( $R^2$ ) with the amount of data used and (b) the variation of mean square error (MSE) with the amount of data used

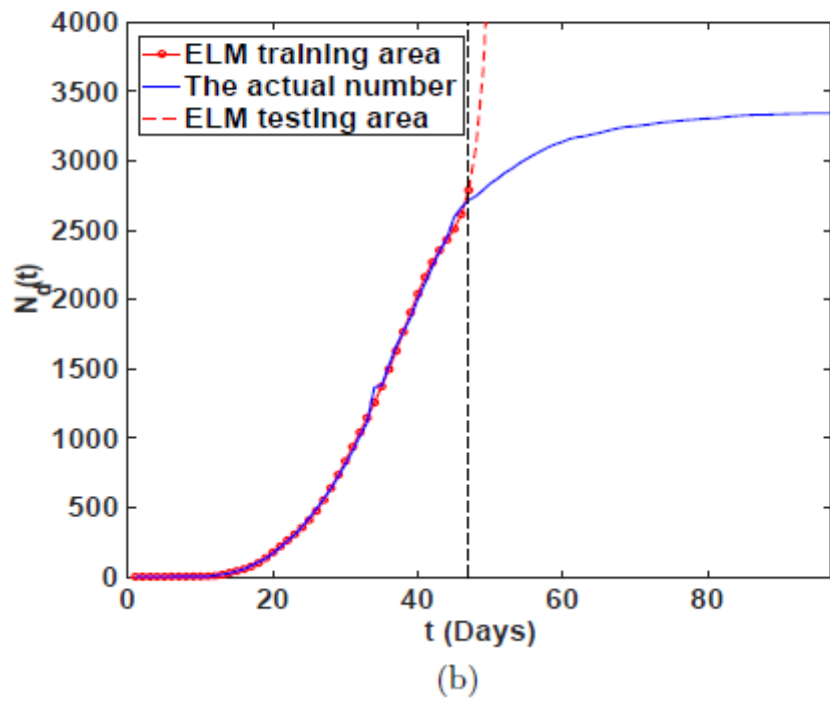
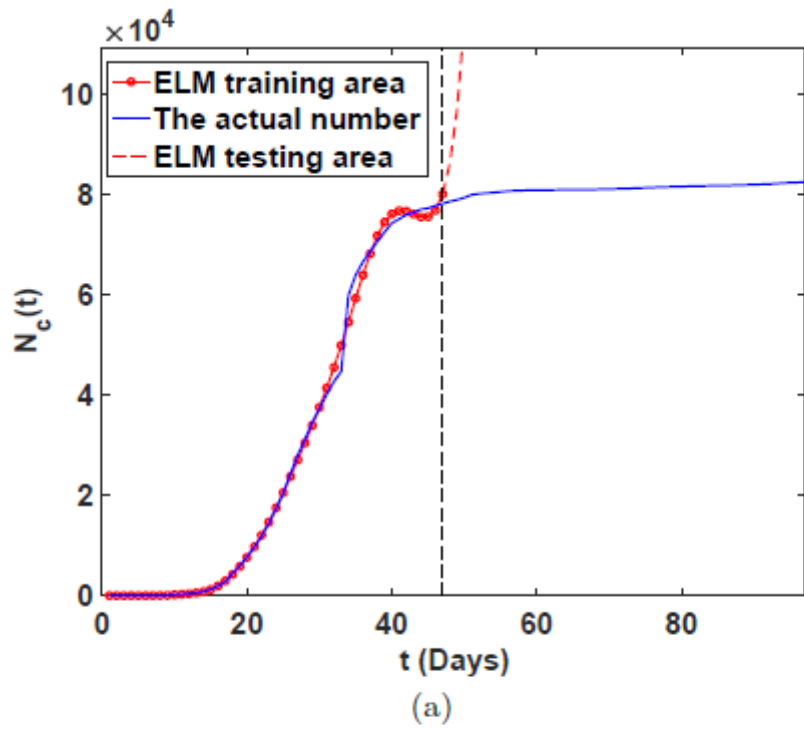


Figure 7

Reconsideration results of Chinese mainland using ELM method followed by (a) the cumulative number of confirmed cases and (b) the cumulative number of deaths

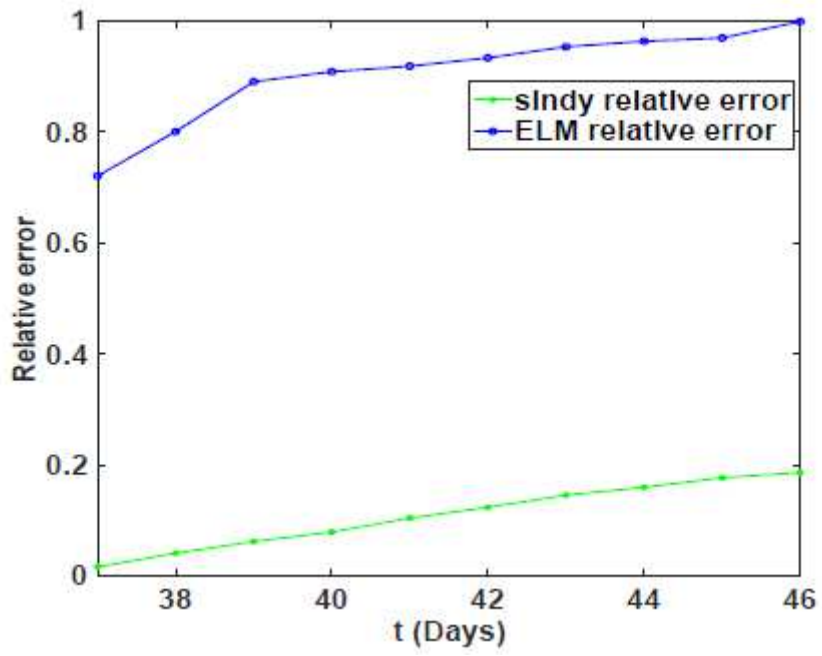


Figure 8

Relative error of the ELM and SINDy-LM methods varies with time